Dalton Transactions

ROYAL SOCIETY OF CHEMISTRY

COMMUNICATION

View Article Online
View Journal | View Issue

Check for updates

Cite this: *Dalton Trans.*, 2020, **49**, 17147

Received 10th October 2020, Accepted 3rd November 2020

DOI: 10.1039/d0dt03507f

rsc.li/dalton

Visible-light-mediated semi-heterogeneous black TiO_2/nickel dual catalytic C (sp^2)–P bond formation toward aryl phosphonates†

Mehdi Koohgard, Haniehsadat Karimitabar and Mona Hosseini-Sarvari *

The combination of black TiO_2 nanoparticles (NPs) with a nickel catalyst provides a low-cost, sustainable, and reusable alternative dual catalytic system to a homogeneous counterpart (noble metals). This black TiO_2-photoredox/nickel dual catalytic system has efficiently driven C–P bond formation between aryl iodides and diarylphosphine oxides under visible light, providing good to excellent yields as well as tolerating a variety of functional groups. The practical application of this semi-heterogeneous protocol has been highlighted by a sunlight experiment, a gram-scale reaction, and a reusability test.

In the last decade, visible-light photoredox catalysis has been a reliable alternative in organic chemistry.[1–6] Recently, dual catalysis based on merging photoredox catalysts with transition-metal catalysts has furnished an alternative strategy in cross-coupling reactions.[7] Started by Sanford's seminal work on arylation of inactivated arenes *via* merging palladium catalyst and photoredox catalyst,[8] various transition metals such as palladium,[9–13] copper,[14–16] gold,[17–23] and rhodium[24,25] have been exploited in the photoredox/metal dual catalysis field. In comparison with the transition-metal counterpart, the combination of photocatalyst with transition-metal catalyst has provided an effective and easily accessible method in C–C and C-heteroatom bond formations under mild conditions. In particular, a great breakthrough was separately obtained by the works of Molander[26] and MacMillan[27] through the combination of (Ir[dF(CF_3)ppy]$_2$(dtbpy))PF_6 and nickel catalysis. They developed a facile strategy for C–C bond formation through a photocatalytic generated alkyl radical intercepted by Ni(II) complexes providing transient access to Ni(III) species (Ni(III)(alkyl)(Ar)) followed by readily reductive elimination to produce a C–C coupled product. Thereafter, more explorations of this dual catalyst system were accomplished to expand the application of photoredox/nickel catalysis to other chemical transformations, especially C-heteroatom bond formation.[28–34] Due to some problems associated with the practical application of iridium or ruthenium polypyridine photocatalysts, quite recently semiconductors as heterogeneous photocatalysts have drawn growing attention in their application in the photoredox/nickel system.[35–38] In comparison with iridium or ruthenium polypyridine, semiconductors are cheap, easy to handle, bench-stable, and recyclable photocatalysts. Recently, some efforts have been devoted to substitute iridium or ruthenium polypyridine complexes with semiconductors in a photoredox/nickel system producing C–N,[37] C–O,[36–38] and C–S[38] bond formation. Nonetheless, there is no report on the application of the semi-heterogeneous photoredox/nickel system in C–P bond formation (Scheme 1).

TiO_2 is well known as a robust, stable, non-toxic, and low-cost heterogeneous photocatalyst in environmental treatment,[39] dye-sensitized solar cells,[40,41] and fuel generations;[42]

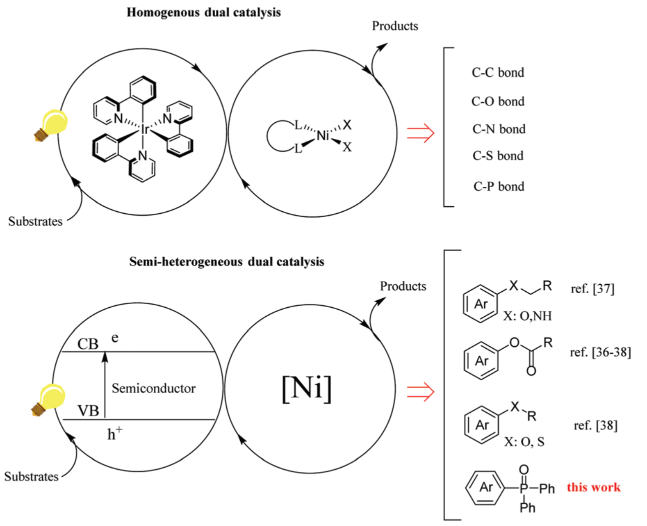

Scheme 1 Homogeneous *vs.* semi-heterogeneous dual Ni photocatalysis.

Shiraz University, Shiraz 7194684795, Islamic Republic of Iran.
E-mail: hossaini@shirazu.ac.ir

† Electronic supplementary information (ESI) available: DETAILS. See DOI: 10.1039/D0DT03507F

however, the ability to forge a TiO_2 semiconductor in photocatalytic organic transformation has been limited due to a relatively large band gap (3.2 eV for anatase and 3.02 eV for rutile)[43] out of the visible light region and rapid recombination of photo-generated charge carriers.[44] To fulfill this aim, some modifications including structural dimensions, *e.g.*, particle size and shape, and electronic structures, *e.g.*, doping, sensitizing, and coupling, have been applied so far.[43,45–49] In 2011, Mao, *et al.* reported a promising alternative approach to enhance the absorption of visible light and even infrared wavelengths through hydrogenation of titania. This new strategy was devised through the generation of disordered nanophase TiO_2 along with hydrogen dopant incorporation.[50] As a consequence, owing to the generation of the mid-gap states and tailing, the band gap of this colored TiO_2 (about 1.54 eV) was noticeably narrowed to be much lower than unmodified TiO_2.[51] Moreover, it exhibited a considerable decrease in the recombination rate of photo-generated electrons and holes due to oxygen vacancy sites which act as electron traps.[51] Since that pioneering work, this type of colored TiO_2 was applied in water splitting and photocatalytic degradation by other research groups.[52–56] Despite these achievements, the application of this colored TiO_2 in organic transformations has been unexplored but is very tempting.

Organophosphine compounds have appeared to be a very significant family of chemicals because of their vast applications in medicinal chemistry, photoelectric materials, material sciences, and catalysis.[57–61] Hence, the introduction of novel catalytic methods to construct C–P bonds has been the subject of current chemistry trends. In the continuation of our recent efforts on developing heterogeneous-based photocatalysis,[43,47,48,62,63] we quite recently reported the first application of black TiO_2 in an organic transformation.[64] We hypothesized that a new synergistic catalytic process might be established in which black TiO_2 will generate P-centered radicals and turn over the nickel catalytic cycle. A possible mechanism for this heterogeneous photoredox/Ni is depicted in Scheme 2. As we illustrated in Scheme 2, the nickel cycle begins with Ni(0). However, the reduction of Ni(II) and Ni(I) to Ni(0) is a different pathway. To begin the catalytic cycle, the nickel catalyst is formed *in situ* from $NiCl_2$(glyme), Ni(II) complex, and dtbbpy (di-*t*-butylbipyridine) in acetonitrile. Black TiO_2 is easily excited under visible light and the corresponding holes abstract one electron from phosphinous acid to produce the cation radical species, followed by deprotonation to provide a P-centered radical. Meanwhile, the conduction band (CB) of black TiO_2 (E^{ox}_{CB} = −2.0 V *vs.* SCE, for pure TiO_2)[65] would be responsible for reducing Ni(II) and Ni(I) complexes to Ni(0) ($E_{1/2}{}^{red}$ [Ni^{II}/Ni^{0}] = −1.2 V *vs.* SCE) and starting the nickel catalytic cycle. Subsequently, the P-centered radical intercepts Ni(II) complexes, resulting from the oxidative addition of the Ni(0) species to aryl halide, and generates an Ni(III) intermediate. This Ni(III) complex might easily undergo reductive elimination to produce the desired product.[26,27,29]

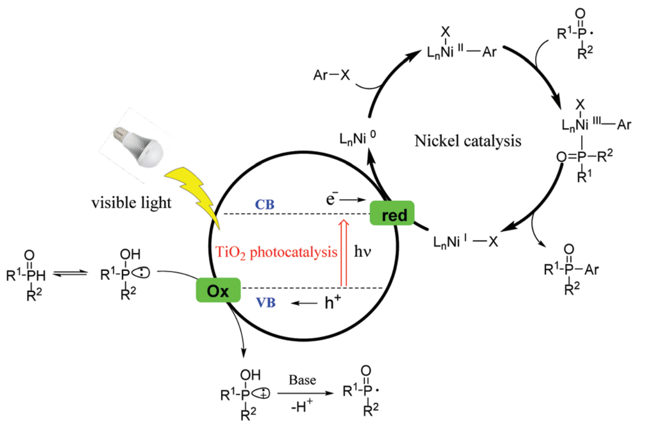

Scheme 2 The proposed reaction mechanism for the dual black TiO_2-photoredox/nickel system.

We commenced our work with the preparation and characterization of black TiO_2 NPs using a previous method[52] (see ESI,† part 2). Afterward, a cross-coupling reaction between 1-iodo-4-methylbenzene (**1a**) and diphenylphosphine oxide (**2a**) served as a model reaction and it was evaluated by using black/white TiO_2 as a photocatalyst, the Ni(II) salt/complex, 4,4′-di-*tert*-butyl-2,2′-dipyridyl (dtbbpy) as the ligand, and several bases under visible light at room temperature. According to the results summarized in Table 1, when the reaction was performed by using $NiCl_2$, MeOH and MeCN turned out to be more efficient solvents (entries 1–6). Notably,

Table 1 Optimization of the reaction conditions[a]

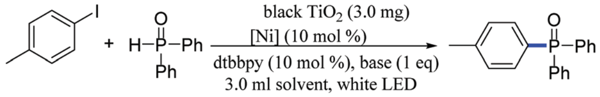

1a 2a 3a

Entry	[Ni]	Solvent	Base	Yield of **3a**[b] (%)
1	$NiCl_2$	DMSO	Cs_2CO_3	9
2	$NiCl_2$	EtOH	Cs_2CO_3	12
3	$NiCl_2$	MeOH	Cs_2CO_3	42
4	$NiCl_2$	$CHCl_3$	Cs_2CO_3	N.D.
5	$NiCl_2$	MeCN	Cs_2CO_3	37
6	$NiCl_2$	THF	Cs_2CO_3	Trace
7	$NiCl_2$·glyme	MeOH	Cs_2CO_3	52
8	$NiCl_2$·glyme	MeCN	Cs_2CO_3	59
9[c]	$NiCl_2$·glyme	MeCN	Cs_2CO_3	91
10[c]	$NiCl_2$·glyme	MeCN	K_2CO_3	72
11[c]	$NiCl_2$·glyme	MeCN	NaOH	29
12[c]	$NiCl_2$·glyme	MeCN	DABCO	47
13[c,d]	$NiCl_2$·glyme	MeCN	Cs_2CO_3	N.D.
14[c,e]	$NiCl_2$·glyme	MeCN	Cs_2CO_3	trace
15[c,f]	$NiCl_2$·glyme	MeCN	Cs_2CO_3	N.D.
16[c]	$NiCl_2$·glyme	MeCN	—	Trace
17[c,g]	$NiCl_2$·glyme	MeCN	Cs_2CO_3	18
18[c]	$Ni(cod)_2$	MeCN	Cs_2CO_3	90

[a] Reaction conditions: 1-iodo-4-methylbenzene (0.5 mmol), diphenylphosphine oxide (0.6 mmol), degassed solvent (3 mL), 3.0 mg photocatalyst, Ni catalyst (10 mol%), dtbbpy (10 mol%), base (1 equiv.) at room temperature, 24 h, under 15 W white LED (λ > 410 nm). [b] Isolated yield. [c] Under Ar (1 atm balloon). [d] No light. [e] No photocatalyst. [f] No Ni catalyst. [g] White TiO_2 (P25). N.D. = not detected.

Table 2 Variation of the substrates[a]

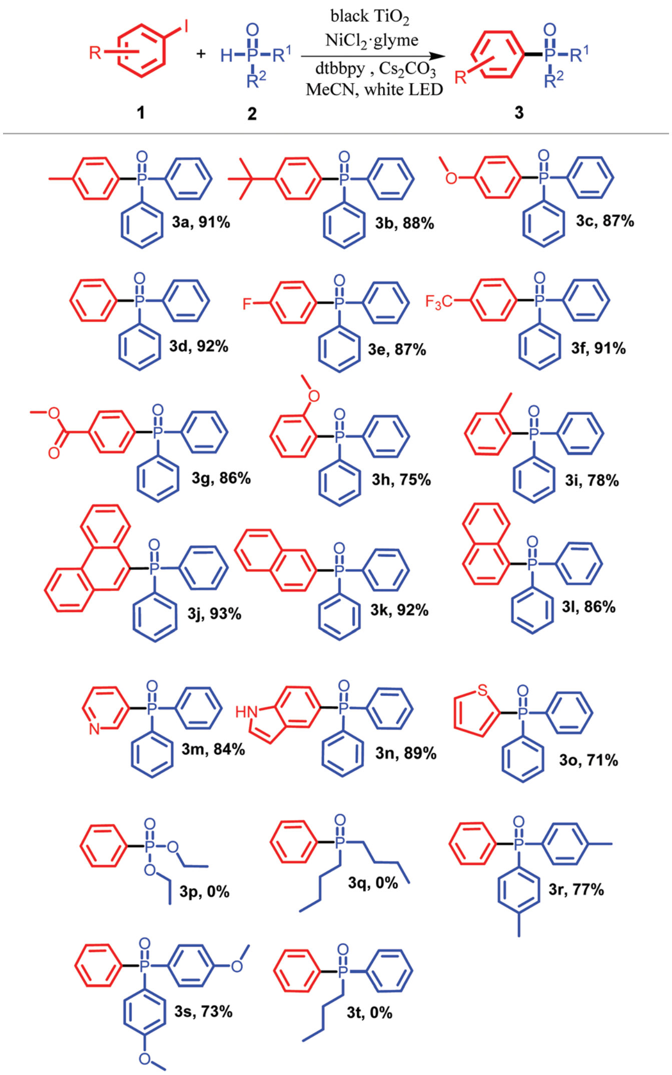

[a] Reaction conditions: **1** (0.5 mmol), **2** (0.6 mmol), black TiO_2 NPs (3.0 mg), $NiCl_2$·glyme (10 mol%), dtbbpy (10 mol%), CS_2CO_3 (1.0 equiv.), and degassed MeCN (3.0 mL) were placed in the vessel and the reaction, under Ar, was stirred at r.t. under 15 W white LED; reaction time was 24 h and the yields were isolated.

the replacement of $NiCl_2$ salt by the more soluble Ni(II) complex ($NiCl_2$·glyme) resulted in considerable improvement of the target product, up to 59% in MeCN (entries 7 and 8). We have further found that removing the oxygen atmosphere from the reaction vessel led to a sharp increase in the reaction efficiency and yielded 91% of **3a** (entry 9). This result might be attributed to an electron transfer between CB of TiO_2 (E^{ox}_{CB} = −2.0 V *vs.* SCE, for pure TiO_2)[65] and molecular oxygen $\left(E^0_{O_2/O_2^{\cdot-}} = -0.8\ \mathrm{V}\ vs.\ \mathrm{SCE}\right)$ [66] which may compete with the reduction cycle of Ni(I) complex to Ni(0) complex, as an essential step in the proposed mechanism. The screening of various bases in this visible-light-mediated dual catalysis revealed that Cs_2CO_3 remained the best choice in the reaction (entries 10–12). Besides, several control experiments were carried out and displayed the presence of light, photocatalyst, nickel catalyst, and base is critical to enabling this reaction (entries 13–16). Moreover, the performance of white TiO_2 (P25) was compared with black TiO_2 NPs under the optimized conditions and only 18% of the corresponding product was isolated after 24 h (entry 17). The generation of the expected product in the presence of white TiO_2 and visible light might come from a small amount of rutile TiO_2 (with lower band gap compared with anatase) in the mixture of TiO_2 as confirmed in the XRD pattern (see ESI, Fig. S2†). Finally, the replacement of Ni(II) complex by $Ni(cod)_2$, as a Ni(0) source, made no meaningful change in the product yield (entry 18, 90%). This might be justified from the fact that the reduction of Ni(II) to Ni(0) at the CB of black TiO_2 NPs is thermodynamically favorable $\left(E^0_{Ni^{II}/Ni^0} = -1.2\ V\ vs.\ \mathrm{SCE}\right)$.[67] However, due to the air and moisture sensitivity of Ni(0) complexes, we preferred to choose $NiCl_2$·glyme as a nickel catalyst in this dual catalytic system.

Next, the variation of substrates was evaluated for this semi-heterogeneous dual catalytic C–P formation under the optimized reaction conditions. As illustrated in Table 2, the reaction is general for a vast number of electron-rich, electron-neutral, and electron-poor substituted groups on aryl iodides such as *tert*-butyl, nitro, ether, and ester moieties (**3a–3i**), providing good to excellent yields. Moreover, the fluorine-containing aryl iodides were tolerated well under these optimal conditions, delivering 87% and 91% of the corresponding products, upon isolation (**3e** and **3f**). Additionally, when the *ortho* position of aryl iodide was occupied with –OMe or –Me, the current procedure resulted in 75% and 78% of the corresponding products, respectively (**3h** and **3i**). This implies that the hindrance effect of the *ortho* position in this reaction was not so important. Considerably, substrates containing fused aromatic ring could also be treated with diphenylphosphine oxide providing the high yields of the target products (**3j–3l**). Notably, this black TiO_2-photoredox/Ni catalytic system could handle heteroaryl iodides containing pyridine, indole, and thiophene in quite acceptable product yields (**3m–3o**). Not surprisingly, the reaction did not proceed toward the production of **3p** and **3q** and the corresponding starting materials remained unchanged. These results come from the high tendency of these types of electron-rich secondary phosphine oxides to be in the form of the pentavalent tautomer,[68,69] and hence this suppresses the photo-oxidation step toward the generation of the P-centered radical in the reaction pathway. Finally, the secondary phosphine oxides bearing –Me and –OMe were applicable under these conditions; however, they produced lower product yields of the corresponding triarylphosphine oxide, that is, in turn, 77% and 73%, respectively (**3r** and **3s**). Also, the reaction did not proceed using butyl(phenyl) phosphine oxide as a substrate (**3t**). Notably, by using aryl bromide and chloride as analogs of aryl iodide, the reaction of these coupling partners with aryl phosphine oxide did not result in the desired product even after 48 h. The lack of reactivity may come from the reduction potential of the corresponding Ni(I)Cl or Ni(I)Br species (after reductive elimination). If their reduction potentials are outside of the required range to be turned over by CB of black TiO_2, the Ni(0) species will not be regenerated in the catalytic cycle to handle the transmetalation step. Moreover, aliphatic iodides (*e.g.*, 1-iodobutane) were tested while surveying the scope of this reaction. The aliphatic halide was not applicable for the synthesis of phosphine oxides of the type $O{=}P(R^1)(R^2)_2$.

Next, to evaluate the synthetic utility of this black TiO_2-photoredox/Ni dual catalytic system, we performed three extra experiments including a sunlight experiment, a scale-up reaction, and reusability of the catalyst. It is noteworthy that black TiO_2 NPs are stable even after 1 year.[52] The photocatalyst maintained efficiency under sunlight and gram-scale experiments as well as during five consecutive runs (see ESI,† part 3).

Then, some control experiments were conducted to get more knowledge about the reaction process. The reaction was quenched in the presence of hole and electron scavengers. Also, the reaction only progressed in the presence of light during an “on/off” LED irradiation experiment. Notably, under the wavelength ranges of white, blue, and green LED lamps (15 W), the product yields were nearly the same, which might be justified by the narrowed band gap of black TiO_2 (2.6 eV). Finally, increasing the irradiation intensity caused a gradual increase in the product yields (see ESI,† part 4).

Conclusions

In summary, a semi-heterogeneous photoredox/Ni dual catalysis system for practical C–P bond formation has been efficiently developed. In this manner, black TiO_2 has been used as a visible-light-driven heterogeneous photocatalyst, instead of the homogeneous counterpart (Ir and Ru), to oxidize phosphinous acid and turn over the nickel cycle in this cross-coupling reaction. The reaction conditions tolerated a vast variety of functional groups on aryl iodide and furnished the corresponding products in good to excellent yields. We believe these results will inspire more studies on the application of black TiO_2 in more organic transformations. This type of modified TiO_2 not only has the advantages of pure TiO_2 such as non-toxicity, chemical stability, low cost, and reusability but also features a narrowed band gap.

Conflicts of interest

There are no conflicts to declare.

Acknowledgements

The authors gratefully acknowledge the support from the Shiraz University Council.

Notes and references

1 X. Zhang, K. P. Rakesh, L. Ravindar and H.-L. Qin, *Green Chem.*, 2018, **20**, 4790–4833.
2 R. Lekkala, R. Lekkala, B. Moku, K. P. Rakesh and H.-L. Qin, *Eur. J. Org. Chem.*, 2019, 2769–2806.
3 Y.-M. Huang, S.-M. Wang, J. Leng, B. Moku, C. Zhao, N. S. Alharbi and H.-L. Qin, *Eur. J. Org. Chem.*, 2019, 4597–4603.
4 X. Zhang, W.-Y. Fang, R. Lekkala, W. Tang and H.-L. Qin, *Adv. Synth. Catal.*, 2020, **362**, 3358–3363.
5 J. Liu, S.-M. Wang and H.-L. Qin, *Org. Biomol. Chem.*, 2020, **18**, 4019–4023.
6 L. Revathi, L. Ravindar, W.-Y. Fang, K. P. Rakesh and H.-L. Qin, *Adv. Synth. Catal.*, 2018, **360**, 4652–4698.
7 K. L. Skubi, T. R. Blum and T. P. Yoon, *Chem. Rev.*, 2016, **116**, 10035–10074.
8 D. Kalyani, K. B. McMurtrey, S. R. Neufeldt and M. S. Sanford, *J. Am. Chem. Soc.*, 2011, **133**, 18566–18569.
9 J. Xuan, T.-T. Zeng, Z.-J. Feng, Q.-H. Deng, J.-R. Chen, L.-Q. Lu, W.-J. Xiao and H. Alper, *Angew. Chem., Int. Ed.*, 2015, **54**, 1625–1628.
10 C. Zhou, P. Li, X. Zhu and L. Wang, *Org. Lett.*, 2015, **17**, 6198–6201.
11 S. Choi, T. Chatterjee, W. J. Choi, Y. You and E. J. Cho, *ACS Catal.*, 2015, **5**, 4796–4802.
12 N. Xu, P. Li, Z. Xie and L. Wang, *Chem. – Eur. J.*, 2016, **22**, 2236–2242.
13 S. K. Bhunia, P. Das, S. Nandi and R. Jana, *Org. Lett.*, 2019, **21**, 4632–4637.
14 I. Perepichka, S. Kundu, Z. Hearne and C.-J. Li, *Org. Biomol. Chem.*, 2015, **13**, 447–451.
15 M. Rueping, R. M. Koenigs, K. Poscharny, D. C. Fabry, D. Leonori and C. Vila, *Chem. – Eur. J.*, 2012, **18**, 5170–5174.
16 Y. Ye and M. S. Sanford, *J. Am. Chem. Soc.*, 2012, **134**, 9034–9037.
17 B. Sahoo, M. N. Hopkinson and F. Glorius, *J. Am. Chem. Soc.*, 2013, **135**, 5505–5508.
18 X.-z. Shu, M. Zhang, Y. He, H. Frei and F. D. Toste, *J. Am. Chem. Soc.*, 2014, **136**, 5844–5847.
19 M. N. Hopkinson, B. Sahoo and F. Glorius, *Adv. Synth. Catal.*, 2014, **356**, 2794–2800.
20 S. Kim, J. Rojas-Martin and F. D. Toste, *Chem. Sci.*, 2016, **7**, 85–88.
21 Y. He, H. Wu and F. D. Toste, *Chem. Rev.*, 2015, **6**, 1194–1198.
22 A. Tlahuext-Aca, M. N. Hopkinson, R. A. Garza-Sanchez and F. Glorius, *Chem. – Eur. J.*, 2016, **22**, 5909–5913.
23 J. Um, H. Yun and S. Shin, *Org. Lett.*, 2016, **18**, 484–487.
24 D. C. Fabry, J. Zoller, S. Raja and M. Rueping, *Angew. Chem., Int. Ed.*, 2014, **53**, 10228–10231.
25 H. J. Kim, D. C. Fabry, S. Mader and M. Rueping, *Org. Chem. Front.*, 2019, **6**, 2319–2323.
26 J. C. Tellis, D. N. Primer and G. A. Molander, *Science*, 2014, **345**, 433–436.

27 Z. Zuo, D. T. Ahneman, L. Chu, J. A. Terrett, A. G. Doyle and D. W. C. MacMillan, *Science*, 2014, **345**, 437–440.

28 E. B. Corcoran, M. T. Pirnot, S. Lin, S. D. Dreher, D. A. DiRocco, I. W. Davies, S. L. Buchwald and D. W. C. MacMillan, *Science*, 2016, **353**, 279–283.

29 T. Kim, S. J. McCarver, C. Lee and D. W. C. MacMillan, *Angew. Chem., Int. Ed.*, 2018, **57**, 3488–3492.

30 M. S. Oderinde, N. H. Jones, A. Juneau, M. Frenette, B. Aquila, S. Tentarelli, D. W. Robbins and J. W. Johannes, *Angew. Chem., Int. Ed.*, 2016, **55**, 13219–13223.

31 C.-H. Lim, M. Kudisch, B. Liu and G. M. Miyake, *J. Am. Chem. Soc.*, 2018, **140**, 7667–7673.

32 J. A. Terrett, J. D. Cuthbertson, V. W. Shurtleff and D. W. C. MacMillan, *Nature*, 2015, **524**, 330–334.

33 E. R. Welin, C. Le, D. M. Arias-Rotondo, J. K. McCusker and D. W. C. MacMillan, *Science*, 2017, **355**, 380–385.

34 J. Xuan, T.-T. Zeng, J.-R. Chen, L.-Q. Lu and W.-J. Xiao, *Chem. – Eur. J.*, 2015, **21**, 4962–4965.

35 C. D. McTiernan, X. Leblanc and J. C. Scaiano, *ACS Catal.*, 2017, **7**, 2171–2175.

36 B. Pieber, J. A. Malik, C. Cavedon, S. Gisbertz, A. Savateev, D. Cruz, T. Heil, G. Zhang and P. H. Seeberger, *Angew. Chem.*, 2019, **58**, 9575–9580.

37 Y.-Y. Liu, D. Liang, L.-Q. Lu and W.-J. Xiao, *ChemComm*, 2019, **55**, 4853–4856.

38 C. Cavedon, A. Madani, P. H. Seeberger and B. Pieber, *Org. Lett.*, 2019, **21**, 5331–5334.

39 M. Pelaez, N. T. Nolan, S. C. Pillai, M. K. Seery, P. Falaras, A. G. Kontos, P. S. M. Dunlop, J. W. J. Hamilton, J. A. Byrne, K. O'Shea, M. H. Entezari and D. D. Dionysiou, *Appl. Catal., B*, 2012, **125**, 331–349.

40 J. Gong, K. Sumathy, Q. Qiao and Z. Zhou, *Renewable Sustainable Energy Rev.*, 2017, **68**, 234–246.

41 V. Sugathan, E. John and K. Sudhakar, *Renewable Sustainable Energy Rev.*, 2015, **52**, 54–64.

42 Y. Ma, X. Wang, Y. Jia, X. Chen, H. Han and C. Li, *Chem. Rev.*, 2014, **114**, 9987–10043.

43 M. Hosseini-Sarvari, Z. Hosseinpour and M. Koohgard, *New J. Chem.*, 2018, **42**, 19237–19244.

44 X. Lang, X. Chen and J. Zhao, *Chem. Soc. Rev.*, 2014, **43**, 473–486.

45 J. Kou, C. Lu, J. Wang, Y. Chen, Z. Xu and R. S. Varma, *Chem. Rev.*, 2017, **117**, 1445–1514.

46 J. Tang, G. Grampp, Y. Liu, B.-X. Wang, F.-F. Tao, L.-J. Wang, X.-Z. Liang, H.-Q. Xiao and Y.-M. Shen, *J. Org. Chem.*, 2015, **80**, 2724–2732.

47 M. Koohgard and M. Hosseini-Sarvari, *Catal. Commun.*, 2018, **111**, 10–15.

48 M. Hosseini-Sarvari, F. Jafari, A. Mohajeri and N. Hassani, *Catal. Sci. Technol.*, 2018, **8**, 4044–4051.

49 X. Lang, X. Chen and J. Zhao, *Chem. Soc. Rev.*, 2014, **43**, 473–486.

50 X. Chen, L. Liu, P. Y. Yu and S. S. Mao, *Science*, 2011, **331**, 746–750.

51 S. Banerjee, S. C. Pillai, P. Falaras, K. E. O'Shea, J. A. Byrne and D. D. Dionysiou, *J. Phys. Chem. Lett.*, 2014, **5**, 2543–2554.

52 H. Tan, Z. Zhao, M. Niu, C. Mao, D. Cao, D. Cheng, P. Feng and Z. Sun, *Nanoscale*, 2014, **6**, 10216–10223.

53 N. Liu, C. Schneider, D. Freitag, M. Hartmann, U. Venkatesan, J. Müller, E. Spiecker and P. Schmuki, *Nano Lett.*, 2014, **14**, 3309–3313.

54 A. Naldoni, M. Allieta, S. Santangelo, M. Marelli, F. Fabbri, S. Cappelli, C. L. Bianchi, R. Psaro and V. Dal Santo, *J. Am. Chem. Soc.*, 2012, **134**, 7600–7603.

55 W. Zhou, W. Li, J.-Q. Wang, Y. Qu, Y. Yang, Y. Xie, K. Zhang, L. Wang, H. Fu and D. Zhao, *J. Am. Chem. Soc.*, 2014, **136**, 9280–9283.

56 Z. Zheng, B. Huang, J. Lu, Z. Wang, X. Qin, X. Zhang, Y. Dai and M.-H. Whangbo, *ChemComm*, 2012, **48**, 5733–5735.

57 A. Skarżyńska, *Coord. Chem. Rev.*, 2013, **257**, 1039–1048.

58 J.-L. Montchamp, *Acc. Chem. Res.*, 2014, **47**, 77–87.

59 C. Queffélec, M. Petit, P. Janvier, D. A. Knight and B. Bujoli, *Chem. Rev.*, 2012, **112**, 3777–3807.

60 C. S. Demmer, N. Krogsgaard-Larsen and L. Bunch, *Chem. Rev.*, 2011, **111**, 7981–8006.

61 S. Van der Jeught and C. V. Stevens, *Chem. Rev.*, 2009, **109**, 2672–2702.

62 S. Firoozi, M. Hosseini-Sarvari and M. Koohgard, *Green Chem.*, 2018, **20**, 5540–5549.

63 Z. Bazyar and M. Hosseini-Sarvari, *J. Org. Chem.*, 2019, **84**, 13503–13515.

64 M. Koohgard and M. Hosseini-Sarvari, *Catal. Sci. Technol.*, 2020, **10**, 6825–6839.

65 M. Cherevatskaya, M. Neumann, S. Füldner, C. Harlander, S. Kümmel, S. Dankesreiter, A. Pfitzner, K. Zeitler and B. König, *Angew. Chem., Int. Ed.*, 2012, **51**, 4062–4066.

66 D. T. Sawyer and J. L. Roberts, *J. Electroanal. Chem.*, 1966, **12**, 90–101.

67 P. N. Bartlett and V. Eastwick-Field, *Electrochim. Acta*, 1993, **38**, 2515–2523.

68 W.-J. Yoo and S. Kobayashi, *Green Chem.*, 2013, **15**, 1844–1848.

69 A. Christiansen, C. Li, M. Garland, D. Selent, R. Ludwig, A. Spannenberg, W. Baumann, R. Franke and A. Börner, *Eur. J. Org. Chem.*, 2010, 2733–2741.